

1987-20188

Neutral Atomic Oxygen Beam
Produced by Ion Charge Exchange for
Low Earth Orbital Simulation

by

Bruce Banks and Sharon Rutledge
NASA Lewis Research Center
Cleveland, Ohio 44135

Marko Brdar, Consultant

Carl Olen and Curt Stidham
Cleveland State University
Cleveland, Ohio 44115

Abstract

A low energy neutral atomic oxygen beam system has been designed and is currently being assembled at the Lewis Research Center. The system utilizes a 15 cm diameter Kaufman ion source to produce positive oxygen ions which are charge exchange neutralized to produce low energy (variable from 5 to 150 eV) oxygen atoms at a flux simulating real time low earth orbital conditions. An electromagnet is used to direct only the singly charged oxygen ions from the ion source into the charge exchange cell. A retarding potential grid is used to slow down the oxygen ions to desired energies prior to their charge exchange. Cryogenically cooled diatomic oxygen gas in the charge exchange cell is then used to transfer charge to the oxygen ions to produce a neutral atomic oxygen beam. Remaining uncharge exchanged oxygen ions are then swept from the beam by electromagnetic or electrostatic deflection depending upon the desired experiment configuration. The resulting neutral oxygen beam of 5-10 cm in diameter impinges upon target materials within a sample holder fixture that can also provide for simultaneous heating and UV exposure during the atomic oxygen bombardment.

Introduction

Many spacecraft materials exposed to the Low Earth Orbital (LEO) environment are oxidized by ram impact of atomic oxygen present as a result of photodissociation of the Earth's upper atmosphere (1-3). The rate of oxidation of most polymers and some metals is sufficiently high to be of concern for LEO space missions. As a result, Space Station must utilize protective coatings or alternative durable materials to assure acceptable long term performance of exposed components such as solar array blankets, composite structures, and solar dynamic power system reflector surfaces (4 and 5).

The development and verification of materials durable to the LEO environment will require both ground based laboratory simulation and in-space testing. The economics and convenience of LEO simulation facilities will result in their extensive use provided there is adequate confidence in their ability to simulate the LEO environment and its effects on materials. The LEO environment is reasonably well characterized in terms of the ram energy and flux of the atomic oxygen which is essentially unionized and in the $3p$

ground state. (See Fig. 1) (1 and 6). However, the laboratory production of $O(3p)$ at these fluxes and energies without the presence of other species not typically present in LEO is difficult. Simulation is even more challenging if one attempts to replicate the synergistic exposure of IR, visible, and UV solar flux; micrometeoroid and space debris impact; thermal cycling; wandering ram vector orientation; and residual upper atmospheric species. Thus one must select those aspects of the LEO environment which are relevant to their particular situation and make arguments that the phenomena occurring in the laboratory simulation adequately replicates that which has been found to occur in LEO. The degree to which an atomic oxygen exposure system credibly simulates the mechanisms occurring in LEO can be judged by quantitative comparison of measurements of the surface texture, chemistry, and erosion yield (mass lost per incident oxygen atom) of a variety of materials that possess volatile oxides. Obviously, the closer one simulates the energy, flux, and species present in the LEO environment, the lower risk of producing effects which do not project a realistic simulation mechanism.

Atomic oxygen can be easily produced at low energies (tenths of an eV) but at high fluxes in RF plasma ashers. Plasma ashers have been valuable for qualitative evaluation of candidate LEO materials. All materials that are known to oxidize in LEO also oxidize in plasma ashers. In addition all materials that are known to be unaffected in space behave the same in plasma ashers. However, the relative rates of oxidation of various materials are not quantifiably in agreement with the LEO results. Thus asher results only allow one to predict that a material will survive or be oxidized in LEO leaving knowledge of the rate of oxidation unknown. This may be a result of differences in energy, flux, metastable states, or species in the plasma. The plasma may contain ions, electrons, diatomic neutrals and atomic neutrals.

This paper presents design considerations for a neutral atomic oxygen beam system currently being assembled at the NASA Lewis Research Center that utilizes ion charge exchange to produce a low energy neutral oxygen beam for LEO simulation.

Vacuum Facility

The vacuum facility layout is shown in Figure 2. It consists of a 60.96 cm diameter by 1.71 m long non magnetic stainless steel chamber to house the neutral atomic oxygen beam system components. The vacuum chamber was specifically designed for the oxygen beam system and has numerous ports for beam characterization probes. It has full diameter access doors at both ends, as well as a large 40.64 cm diameter port to mount a vertically downward oriented ion source within it. The cylindrical vacuum chamber is evacuated by a 25.4 cm diameter 2350 l/sec diffusion pump with its associated cold trap and roughing pump. The pumping system utilizes fomblinized oil to allow chemical stability when pumping oxygen.

Ion Source

The ion source, shown schematically in Figure 3 is a 15 cm diameter electron bombardment ion source. The ion source is used to produce oxygen ions which are to be neutralized by charge exchange as shown in Figure 4. The ion source utilizes a hot wire filament cathode in which Pt or Ir will be used to insure adequate life in the oxygen environment. The ion source will be

operated with one of three candidate gases: O_2 , N_2O , or CO_2 , depending upon their overall system performance. Molecular oxygen is an ideal source gas in that it does not introduce contaminant gases into the vacuum facility. However, as can be seen in Table I there are numerous excited states of O^+ that would potentially be present and thus accelerated as part of the ion beam. Ideally one would like only the $O^+(4S)$ ground state ions to be generated in the ion source discharge chamber. However, it is anticipated that ions produced will be 75% O_2^+ and 25% O^+ , where the O^+ is comprised of both ground state and metastable states (8).

Measurements of electron impact ionization of O_2 by Neynaber and Magnuson (7) have indicated that the single ions are composed of 65% $O^+(4S)$ ground state ions; and 25% $O^+(2D)$ and 10% $O^+(2P)$ metastable ion states. N_2O and CO_2 source gasses have the potential advantage of producing significantly higher percentages of ground state oxygen ions but have the added complication of introduction of unwanted ion and neutral species.

The ions produced within the discharge chamber are accelerated by the ion optics shown in Figure 3. The energy distribution of the accelerated ions is more dependent upon the potential gradients within the discharge chamber than the applied accelerating potential which can be accurately set. The small potential gradients within the discharge chamber are expected to produce energy uncertainties of the order of 1eV. Depending upon the choice of ion optics (one, two, or three grids) the oxygen ions will then be accelerated to specific energies up to 150 eV. Single accelerator grid ion optics allows very high current densities to be extracted at low ion energies (9). Average ion current densities of 7 mA/cm² have been measured for 50 eV argon ions (10). Single ion optics typically consist of a high open area electroformed metal mesh (usually gold or nickel) which is negatively biased. The mesh spacing is chosen to be smaller than the space charge limited flow acceleration sheath distance. Single grid optics enable high current density ion beams to be produced at low net ion energies which allows the use of lower magnetic fields for beam manipulation. However, the single grid ion beams appear to be quite divergent at these low energies. Two grid ion optics, in which the most upstream grid (the screen grid) is at ion source cathode potential and the downstream grid (the accelerator grid) is negatively biased, must be operated at higher net ion energies to achieve reasonable current densities but their beams are much better aligned. Three grid ion optics utilize the two grid optics but have an additional downstream grounded grid which reduces beam divergence when operated at low voltages with high current densities. The two and three grid optics generally consist of a hexagonal array of 1 to 2 mm diameter apertures in 0.4 mm thick dished molybdenum sheets separated by 0.3-0.5 mm gaps. Final choice of the ion optics type will depend upon their relative ability to provide high current density at the inlet of the charge exchange cell.

The ion beam produced by the ion source is then neutralized (in a bulk plasma sense but not microscopically) by the addition of electrons from a hot wire neutralizer located just downstream of the ion source.

Ion Selecting Magnet

An electromagnet is used to direct the singly charged oxygen ions toward the charge exchange cell as shown in Figures 4 and 5. The electromagnet also

serves to selectively reject O_2^+ and any O^{++} ions from entering the charge exchange cell. The electromagnet is large enough to bend the full 15 cm diameter beam at energies up to 150 eV with a .0415 tesla field in its gap.

Charge Exchange Cell and Retarding Screen

The singly charged oxygen enters a charge exchange cell after first being slowed by passing through a retarding screen shown in Figures 4 and 5. The screen cage within the charge exchange cell is biased to a positive potential such that the net ion energy has been slowed to 4-5 eV. Because positively biased surfaces tend to draw high electron currents it may be necessary to provide a negatively biased electron repeller screen just upstream of the positively biased ion retarding screen. The termination of electron flow along with the ion flow would necessitate their readdition by means of a neutralizer filament within the charge exchange cell cage. Inside the charge exchange cell a low temperature charge transfer gas is present to supply electrons to the oxygen ions and thus produce a fast 4-5 eV oxygen atom beam. Ideally one would like the reaction $O^+(4S) + O_2 \rightarrow O(3p) + O_2$ to occur with a high probability and without trajectory alterations. The probability of charge transfer is increased if one increases the density of the charge transfer gas, as well as, increasing the length of the cell. The cell shown in Figure 5 is ≈ 50 cm long. The O_2 gas density in the cell is elevated by cryogenically cooling its copper walls. The cross-section for $O^+ + O_2 \rightarrow O + O_2^+$ is approximately 2×10^{-16} cm² for ground state ions and 3×10^{-15} cm² for metastable ions (11). Based on this charge exchange cell size, the ground state charge transfer cross-section, and an O_2 pressure of 10^{-4} torr, approximately 31% of the incoming ions will be converted to neutral oxygen atoms.

Several charge transfer issues invite the consideration of alternate gases and alternate configurations. The highest probability charge transfer occurs from resonant transfer with atomic oxygen. Because of the complexity of obtaining a high population of cold atomic oxygen one might consider other gases with larger Franck-Condon overlaps with $O^+(4S)$ at the recombination energy (13.618 eV). Gases which appear to have a high probability of momentumless charge transfer include H_2O , CO_2 , CH_2F_2 and CF_4 (12). However, each of these gases will allow nonoxygen species to be back ingested into the ion source thus allowing some probability of their ionization and subsequent acceleration. In the case of CO_2 , back injection may not be a problem if CO_2 is also used as the ion source gas.

The exact degree to which charge transfer can occur with various gases without momentum transfer is not well characterized for oxygen ion beams of 4-5 eV. If the charge transfer occurs and imparts significant trajectory changes to the oxygen ions then a very short single open ended charge exchange cell operated at high pressure would be needed to allow acceptable fluxes to arrive at the target sample surface. A short 5.08 cm long, charge exchange cell option is being fabricated with a small variable diameter entrance hole. The cell utilizes an electrostatic repeller screen to prevent uncharge exchanged ions from impacting the sample surface. The reduced inlet to the cell and lack of an exit port will allow much higher number densities to be achieved within the cell and still enable off axis directed atomic oxygen to impinge on the target sample surfaces.

Ion Deflector Magnet

Uncharge exchanged ions are bent 90° downward from the atomic oxygen beam by an electromagnet located just downstream of the charge exchange cell to prevent their impingement upon the sample surface. This electromagnet will be operated to produce a 0.0076 tesla field over its 12 cm gap.

Sample Holder & Environment

The atomic oxygen impinges upon target samples located just downstream of the ion deflector magnet. The goal of the system is to simulate the atomic oxygen flux (10^{11} - 10^{14} oxygen atoms/cm² sec) and energy (4.2 - 4.4 eV) of LEO conditions, as well as the UV and thermal environment. Thus the samples are located in a thermally controlled box with the capability of synergistic UV exposure as shown in Figure 6. Sample rotation is also possible to correctly simulate the changing angle of attack that would occur on solar oriented surfaces.

Simulation Analysis

The energy characterization of the atomic oxygen beam can be inferred by means of retarding potential probing of the oxygen ions which have not charge exchanged. The measurement of the atomic oxygen flux can be accomplished by comparative pressure measurements of a differentially pumped cavity located in the target sample plane. An inlet aperture in the cavity allows both the O₂ from the background vacuum facility and the atomic oxygen to enter a pumped chamber. Because the O₂ is randomly directed it has a high probability of being pumped out while the axially directed atomic oxygen exits through a downstream aperture and enters an absolute pressure measurement cavity. By comparing the pressure in this cavity for beam on and beam off conditions via turning on and off the ion selecting magnet a flux through the sample plane can be calculated.

Because erosion rates of materials exposed to expected Space Station altitude fluxes is low, thin film surface analysis techniques including Rutherford backscattering will be utilized to measure material erosion yields.

Concluding Remarks

A low energy atomic oxygen beam system designed to simulate both the energy and flux of the LEO environment is being assembled at the NASA Lewis Research Center. A variety of design considerations and configuration options are being considered to optimize the quality of the simulation. Synergistic thermal, UV, and angle of attack exposure considerations will be provided with surface analysis techniques used to quantify material loss rates.

Acknowledgements

The authors gratefully acknowledge the helpful suggestions provided by Dr. Jean Futrell of University of Delaware, Dr. Harold Kaufman of Front Range Research and Dr. Paul Wilbur of Colorado State University.

References

1. B. Banks, M. Mirtich, S. Rutledge, and H. Nahra, "Protection of Solar Array Blankets from Attack by Low Earth Orbital Atomic Oxygen," paper presented at the 18th IEEE Photovoltaic Specialists Conference, Las Vegas, NV, Oct. 21-25, 1985.
2. L. Leger, "Oxygen Atom Reaction with Shuttle Materials at Orbital Altitudes," NASA TM-58246, 1982.
3. A. Whitaker, "LEO Atomic Oxygen Effects on Spacecraft Materials," paper presented at the AIAA Shuttle Environment and Operations Meeting, Washington, D.C., Oct. 31-Nov. 2, 1983, AIAA-83-2632-CP.
4. B. Banks, M. Mirtich, S. Rutledge, D. Swec, and H. Nahra, "Ion Beam Sputter-Deposited Thin Film Coatings for Protection of Spacecraft Polymers in Low Earth Orbit," NASA TM 87051, Jan., 1985.
5. D. Gulino, R. Egger, and W. Banholzer, "Oxidation-Resistant Reflective Surfaces for Solar Dynamic Power Generation in Near Earth Orbit," paper presented at the 33rd National Symposium of the American Vacuum Society, Baltimore, MD, Oct. 27-31, 1986.
6. L. Leger, J. Visentine, and J. Schliesing, "A Consideration of Atomic Oxygen Interactions with Space Station," AIAA paper 85-0476, Jan., 1986.
7. R. H. Neynaber and G. D. Magnuson, "Associative Ionization in Collisions between Metastable Helium and Atomic Nitrogen and Oxygen," J. Chem. Phys., Vol. 64, No. 7, April 1, 1976.
8. P. Wilbur, Colorado State University, personal communication.
9. J. Harper, J. Cuomo, and H. Kaufman, "Technology and Applications of Broad-beam Ion Sources Used in Sputtering, Part II Applications," J. Vac. Sci. Technol., Vol. 21, No. 3, Sept./Oct., 1982.
10. J. R. Sovey, NASA Lewis Research Center, personal communication.
11. M. Bortner and T. Baurer, "Defense Nuclear Agency Reaction Rate Handbook," Second Edition, DNA 1984H, Revision No. 8, April, 1979.
12. J. Futrell, University of Delaware, personal communication.

Table I - Oxygen Atom and Ion States

STATE	ENERGY (eV)	MEAN RADIATIVE LIFETIME (SEC)
0 (3P)	Ground State	∞
0 (1S)	4.18	.8
0 ($3s^5S^0$)	9.13	.0006
0 ($3s^3S^0$)	9.51	1.8×10^{-9}
0 (1D)	1.96	148.00
0 ⁺ (4S)	Ground State	∞
0 ⁺ ($^2D^0_{3/2}$)	3.33	5.9×10^3
0 ⁺ ($^2D^0_{5/2}$)	3.32	2.1×10^4
0 ⁺ ($^2P^0_{1/2}$)	5.01	5.4
0 ⁺ ($^2P^0_{3/2}$)	5.01	4.2

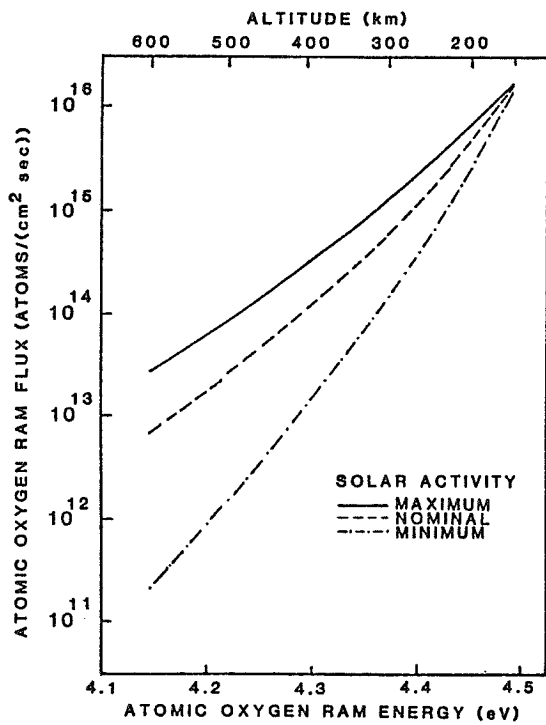


Fig. 1 - Atomic oxygen ram flux and energy as a function of altitude.

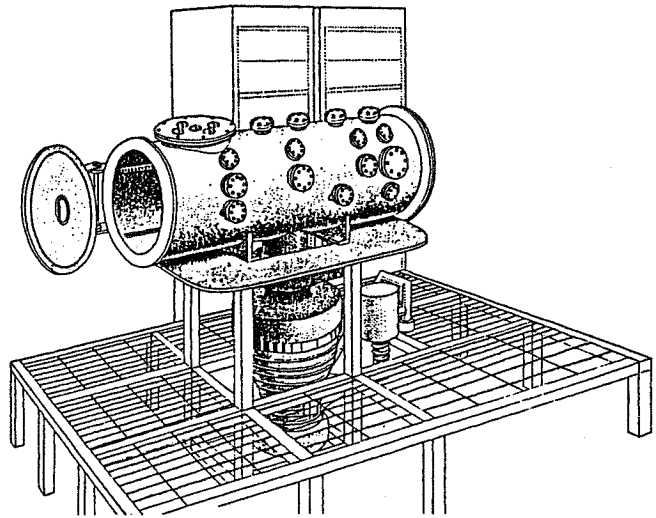


Fig. 2 - Atomic oxygen beam vacuum facility.

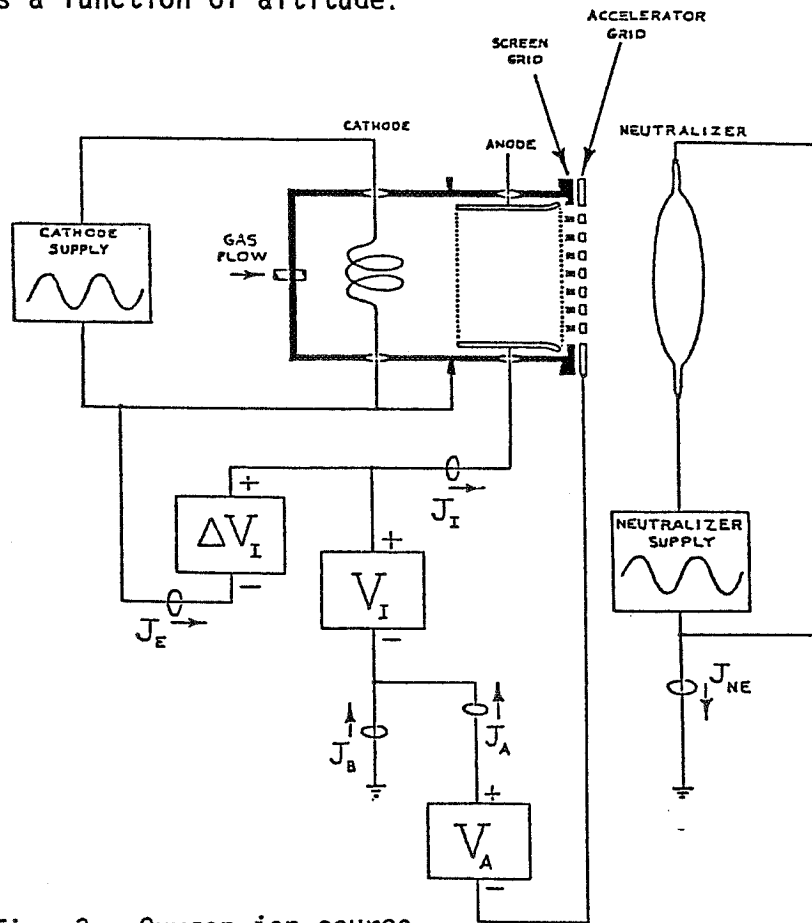


Fig. 3 - Oxygen ion source.

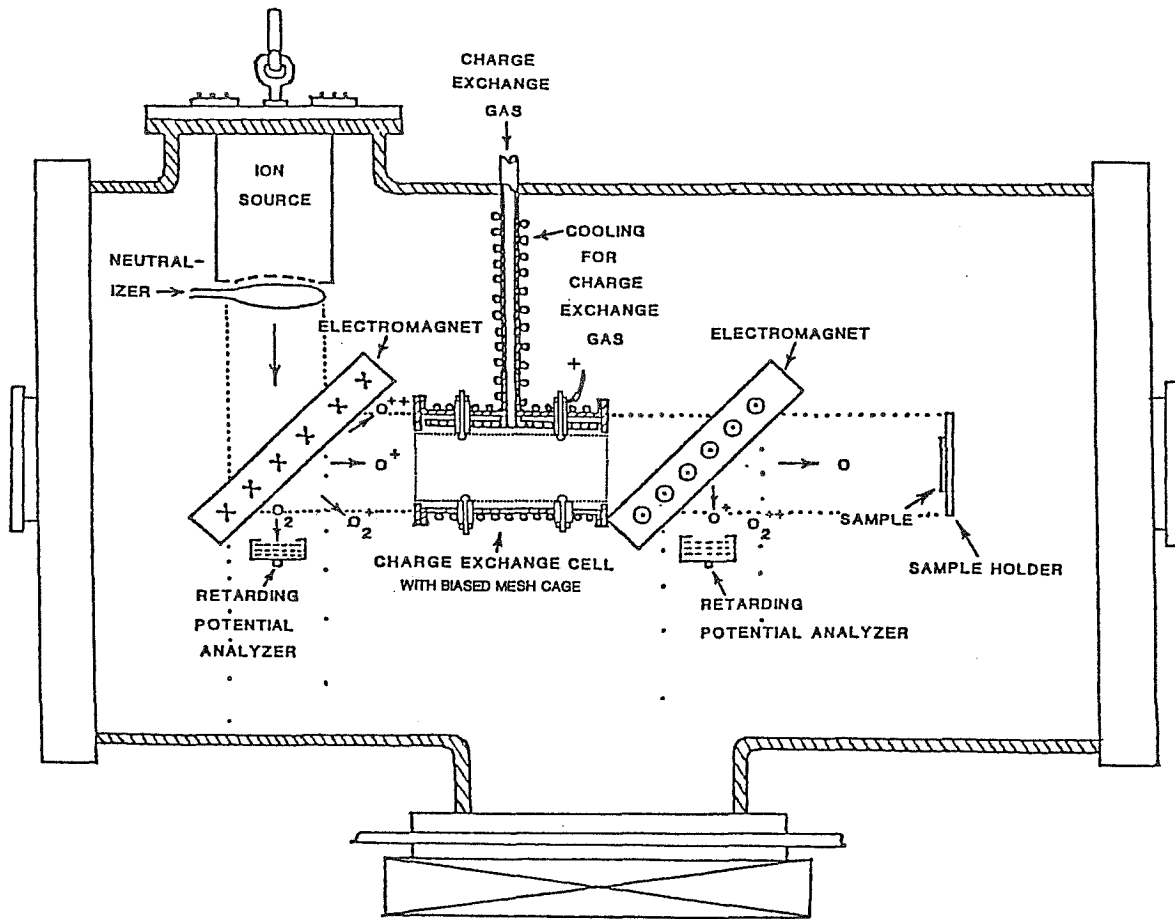


Fig. 4 - Overall schematic of atomic oxygen beam system.

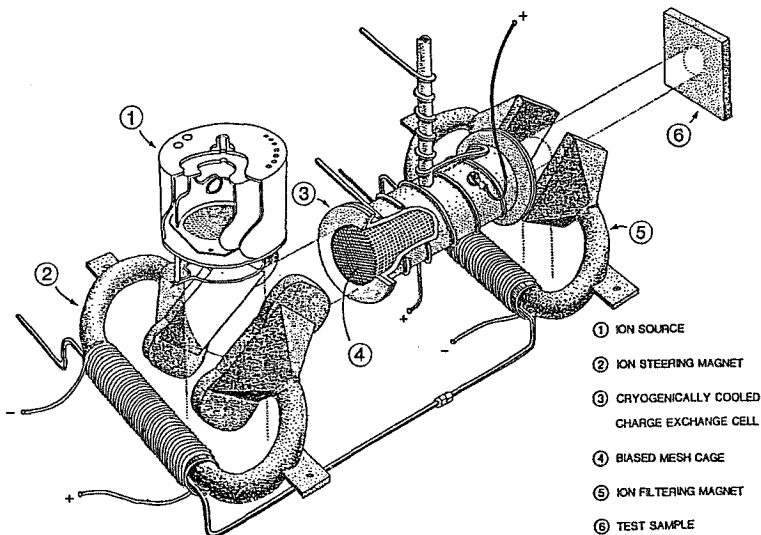


Fig. 5 - Sketch of atomic oxygen beam system components.

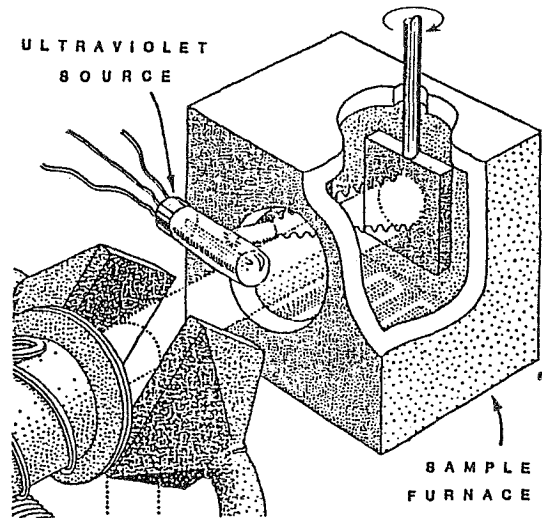


Fig. 6 - Target sample holder configuration.